

# Conjugated polymers based on C, Si and N-bridged dithiophene and thienopyrroledione units: synthesis, field-effect transistors and bulk heterojunction polymer solar cells

Yong Zhang, Jingyu Zou, Hin-Lap Yip, Ying Sun, Josh A. Davies, Kung-Shih Chen, Orb Acton and Alex K.-Y. Jen\*

Received 15th November 2010, Accepted 4th December 2010

DOI: 10.1039/c0jm03927f

A series of low band-gap conjugated polymers (PDTC, PDTSi and PDTP) containing electron-rich C-, Si-, and N-bridged bithiophene and electron-deficient thienopyrroledione units were synthesized *via* Stille coupling polymerization. All these polymers possess a low-lying energy level for the highest occupied molecular orbital (HOMO) (as low as  $-5.44$  eV). As a result, photovoltaic devices derived from these polymers show high open circuit voltage ( $V_{oc}$  as high as 0.91 V). These rigid polymers also possess respectable hole mobilities of  $1.50 \times 10^{-3}$ ,  $6.0 \times 10^{-4}$ , and  $3.9 \times 10^{-4}$   $\text{cm}^2 \text{V}^{-1} \text{s}^{-1}$  for PDTC, PDTSi, and PDTP, respectively. The combined high  $V_{oc}$  and good hole mobility enable bulk heterojunction photovoltaic cells to be fabricated with relatively high power conversion efficiency (PCE as high as 3.74% for the PDTC-based device).

## 1. Introduction

Bulk hetero-junction-based (BHJ) polymer photovoltaic cells have been vigorously investigated due to their potential for high-speed processing using roll-to-roll printing to meet the scalability challenge for low-cost renewable energy.<sup>1-4</sup> The most frequently studied BHJ cells involve the blending of a conjugated polymer (electron donor) and a fullerene derivative (electron acceptor) to form a nanoscale interpenetrating network to serve as the active layer. The morphology of this active layer can be optimized by either solvent or thermal annealing using mixed solvents or additives.<sup>5-10</sup> For example, the regioregular poly(3-hexylthiophene) (P3HT) based devices have been demonstrated to be able to achieve  $\sim 5\%$  power conversion efficiency (PCE) using these methods.<sup>9,11</sup> However, the relatively large band-gap and high HOMO energy level of P3HT limit the possibility of further improving device performance. More recently, significant progress has been made in new material development to enable devices with very high PCEs ( $\geq 7\%$ ).<sup>12-17</sup> In order to obtain higher PCE, the short circuit current ( $J_{sc}$ ), open circuit voltage ( $V_{oc}$ ), and fill factor (FF) of the device need to be optimized simultaneously.<sup>1</sup> The  $J_{sc}$  is correlated to the absorption of the active layer, therefore, better matched absorption with the solar spectrum will potentially give higher  $J_{sc}$ .  $V_{oc}$  is mainly determined by the energy offset between the HOMO of the polymer donor and the lowest unoccupied molecular orbital (LUMO) of the fullerene derivatives, although the interface between the

corresponding electrodes can also affect  $V_{oc}$ .<sup>18-20</sup> As a result, it is very critical to develop polymers with small band-gap and good hole mobility, while maintaining a low lying HOMO energy level to ensure high  $V_{oc}$ .

Compared to conjugated homopolymers (such as P3HT), donor-acceptor (D-A) conjugated polymers, with electron-rich and electron-deficient units alternating on the polymer backbone, are proven to be an effective approach to make low band-gap polymers. The band-gap and energy level of these conjugated polymers can be easily tuned by using suitable donor and acceptor units, such as fluorene, silafluorene, carbazole, benzo-dithiophene, benzothiadiazole, quinoxaline, and thienopyrazine, *etc.*, to achieve PCE of higher than 5%.<sup>7,8,12-17</sup>

Among these conjugating moieties, a dithiophene unit bridged with a carbon (C) or a silicon (Si) atom has been incorporated into alternating copolymers with an electron-deficient benzothiadiazole unit to make efficient polymer BHJ cells.<sup>10,21</sup> Originally, a low PCE of *ca.* 2.7% was achieved for devices containing the C-bridged dithiophene-based polymer donor (PCPDTBT) and the PC<sub>61</sub>BM acceptor.<sup>21</sup> By optimizing the morphology of the PCPDTBT/PC<sub>71</sub>BM blend with a small amount of alkylendithiol additive, the PCE went up to 5.5%.<sup>10</sup> However, other conjugated polymers with the same donor unit can only get low PCE of 1-2%.<sup>22,23</sup> This shows that the morphologies of these types of polymers are quite sensitive to the solvents or additives used for device processing. In addition to PCPDTBT, its Si analog, PSBTBT, has also been reported by Hou *et al.*<sup>17</sup> and Brabec *et al.*<sup>24</sup> as a promising polymer donor for PSCs. By changing the bridging atom from C to Si, the PCE of the devices can improve to 5.1% without adding any additives during the device fabrication.<sup>17</sup> This is possible because the longer C-Si

Department of Materials Science and Engineering, University of Washington, Seattle, Washington, 98195, USA. E-mail: ajen@u.washington.edu; Fax: +1 206 543 3100; Tel: +1 206 543 2626

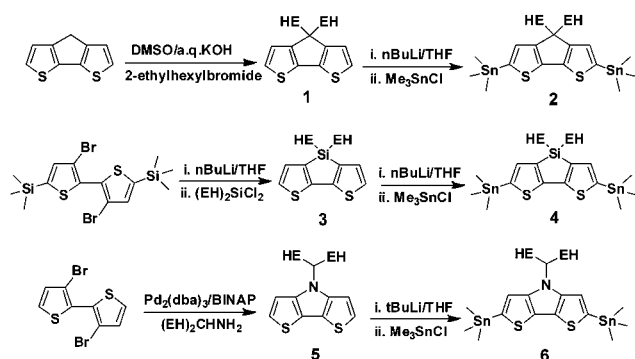
bond ( $\sim 0.3$  Å) on PSBTBT allows for better inter-chain polymer packing to improve hole mobility. Compared to the C- and Si-bridged dithiophene, dithieno[3,2-*b*:2',3'-*d*]pyrrole (DTP), the N-bridged dithiophene, possesses stronger electron-donating ability and has been used as an electron-rich donor for D–A conjugated polymers. For example, DTP-based polymers such as PDTPDTBT and PDTPDTPDPP containing either bis(2-thienyl)-2,1,3-benzothiadiazole-5',5''-diyl or a 3,6-dithiophen-2-yl-2,5-dihydropyrrolo[3,4-*c*]pyrrole-1,4-dione (DPP) as the electron-deficient unit have been reported by Zhou *et al.* that show broad absorption almost reaching 1100 nm. However, BHJ cells derived from these polymers only show relatively low PCE of 2.18% and 2.71%.<sup>25,26</sup> This is due to the low  $V_{oc}$  (0.37–0.62 V) of these devices (as a result of high HOMO energy level of these polymers) that limits their performance. Therefore, it is critical to develop polymers with optimal HOMO energy levels and charge-transporting properties to improve device performance.

In this paper, we present a series of new D–A alternating polymers based on C-, Si- and N-bridged dithiophene as the electron-rich donor and thienopyrroledione (TPD) as the electron-deficient acceptor. Recently, we and others have reported devices based on polymer containing thienopyrroledione (TPD) and benzodithiophene units that show high  $V_{oc}$  (as high as 0.89 V).<sup>27–30</sup> This inspires us to further explore the possibility of using TPD to copolymerize with electron-rich bridged dithiophenes to improve polymer properties. These polymers were synthesized *via* a Stille coupling polymerization reaction (Scheme 1 and 2). The optical, electrochemical, charge-transporting, and photovoltaic properties have been investigated. The results from electrochemical studies showed that these polymers have relatively low HOMO energy levels of *ca.* –5.40 eV, therefore,  $V_{oc}$  of the photovoltaic cells derived from these materials is as high as 0.91 V, which is among the highest obtained for bridged dithiophene-based polymer photovoltaic devices.

## 2. Experimental section

### Materials and general characterization method

All reagents were purchased from commercial sources without further purification. 4*H*-Cyclopenta[2,1-*b*:3,4-*b'*]dithiophene, 4,4-di(2-ethylhexyl)-4*H*-cyclopenta[2,1-*b*:3,4-*b'*]dithiophene (**1**), 3,3'-dibromo-5,5'-bis(trimethylsilyl)-2,2'-bithiophene, 4,4'-bis-



Scheme 1 Synthetic route for monomers.

(2-ethylhexyl)-dithieno[3,2-*b*:2',3'-*d*]silole (**3**), 3,3'-dibromo-2,2'-bithiophene, *N*-[1-(2'-ethylhexyl)-3-ethylheptanyl]-dithieno[3,2-*b*:2',3'-*d*]pyrrole (**5**) and 5-octylthieno[3,4-*c*]pyrrole-4,6-dione were prepared by following literature procedures.<sup>25,31,32</sup> UV-Vis spectra were obtained using a Perkin-Elmer Lambda-9 spectrophotometer. The <sup>1</sup>H NMR spectra were collected on a Bruker AV 300 or 500 spectrometer operating at 300 or 500 MHz in deuterated chloroform solution with TMS as reference. Cyclic voltammetry of polymer films was conducted in acetonitrile with 0.1 M of tetrabutylammonium hexafluorophosphate using a scan rate of 100 mV s<sup>-1</sup>. ITO, Ag/AgCl and Pt mesh were used as working electrode, reference electrode and counter electrode, respectively. Differential scanning calorimetry (DSC) was performed using a DSC2010 (TA instruments) under a heating rate of 10 °C min<sup>-1</sup> and a nitrogen flow of 50 mL min<sup>-1</sup>. GPC and preparative GPC were performed on a Waters 410 differential refractometer with two columns connected in series with a THF (the mobile phase) flowing rate of 1 mL min<sup>-1</sup>. Monodisperse polystyrene samples were used as the standard for the determination of molecular weight. AFM images under tapping mode were taken on a Veeco multimode AFM with a Nanoscope III controller.

### Device fabrication and characterization

To fabricate conventional configuration solar cells, ITO-coated glass substrates (15 Ω sq<sup>-1</sup>) were first cleaned with detergent, deionized water, acetone, and isopropyl alcohol. A thin layer (*ca.* 40 nm) of PEDOT:PSS (Baytron® P VP AI 4083, filtered at 0.45 μm) was first spin-coated on the pre-cleaned ITO-coated glass substrates at 5000 rpm and baked at 140 °C for 10 min under ambient conditions. The substrates were then transferred into an argon-filled glove-box. Subsequently, the polymer:PC<sub>71</sub>BM active layer (*ca.* 90 nm) was spin-coated onto the PEDOT:PSS layer at 900 rpm from a homogeneous blend solution. The solution was prepared by dissolving the polymer at a blend weight ratio of 1 : 2 in *o*-dichlorobenzene (or *o*-dichlorobenzene with 2 vol% of 1-chloronaphthalene) and filtered with a 0.2 μm PTFE filter. At the final stage, the substrates were pumped under high vacuum ( $< 2 \times 10^{-6}$  Torr), and calcium (0.8 nm) topped with aluminium (100 nm) was thermally evaporated onto the active layer through a shadow mask to define the active area of the devices. The device pattern was a 2 mm diameter circle, which had nominal device area of  $3.14 \times 10^{-2}$  cm<sup>2</sup>. The un-encapsulated solar cells were tested under ambient conditions using a Keithley 2400 SMU and an Oriel Xenon lamp (450 W) with an AM1.5 filter. A mask was used to define the device illumination area of 10.08 mm<sup>2</sup> to minimize photocurrent generation from the edge of the electrodes. The light intensity was calibrated to 100 mW cm<sup>-2</sup> using a calibrated silicon solar cell with a KG5 filter, which had been previously standardized at the National Renewable Energy Laboratory.

### Synthesis

**Compound 2.** To a solution of compound **1** (230 mg, 0.57 mmol) in THF (10 mL) was added *n*-BuLi (1 mL, 2 M in hexane) at –78 °C. The resulting mixture was kept at –78 °C for 30 min then at room temperature for 30 min. After cooling to –78 °C,

trimethyltin chloride (1.5 mL, 1 M in hexane) was added in one portion. The mixture was poured into water after stirring at room temperature overnight and extracted with hexane. The organic phase was dried over anhydrous  $\text{Na}_2\text{SO}_4$ . After removing the solvent under vacuum, a black liquid was achieved and used in the next step without further purification (280 mg, 67%).  $^1\text{H NMR}$  (300 MHz,  $\text{CDCl}_3$ ,  $\delta$ ) 6.96 (t, 2H), 1.86 (m, 4H), 1.02–0.93 (m, 18H), 0.76 (t,  $J = 6.5$  Hz, 6H), 0.60 (t,  $J = 7.3$  Hz, 6H), 0.37 (t, 18H). HRMS (ESI,  $m/z$ ):  $[M + \text{H}]^+$  calcd for  $\text{C}_{31}\text{H}_{54}\text{S}_2\text{Sn}_2$ , 730.1711; found, 730.1699.

**Compound 4.** Compound 4 was prepared by following the similar procedure for making compound 2 from compound 3 in a yield of 77%.  $^1\text{H NMR}$  (300 MHz,  $\text{CDCl}_3$ ,  $\delta$ ) 7.09 (s, 2H), 1.43 (m, 4H), 1.31–1.16 (m, 18H), 0.84–0.76 (m, 12H), 0.39 (s, 18H).

**Compound 6.** To a solution of compound 5 (300 mg, 0.72 mmol) in THF (15 mL) was added *t*-BuLi (1 mL, 1.7 M in hexane) at 0 °C. The resulting mixture was kept at 0 °C for 1 h. Trimethyltin chloride (2 mL, 1 M in hexane) was added in one portion. The mixture was poured into water after stirring at room temperature overnight and extracted with hexane. The organic phase was dried over anhydrous  $\text{Na}_2\text{SO}_4$ . After removing the solvent under vacuum, a yellow liquid was achieved and used in the next step without further purification (400 mg, 75%).  $^1\text{H NMR}$  (300 MHz,  $\text{CDCl}_3$ ,  $\delta$ ) 7.00 (s, 2H), 4.48 (m, 1H), 2.12 (m, 2H), 1.63 (m, 2H), 1.22–0.60 (m, 30H), 0.38 (s, 18H).

**1,3-Dibromo-5-octylthieno[3,4-*c*]pyrrole-4,6-dione (7).** To a solution of 5-octylthieno[3,4-*c*]pyrrole-4,6-dione (0.5 g, 1.9 mmol) in trifluoroacetic acid (5 mL) and conc.  $\text{H}_2\text{SO}_4$  (2 mL) was added NBS (1.1 g, 6.2 mmol) in portions. The mixture was stirred at room temperature overnight. Then, water (50 mL) was added and the mixture was extracted with dichloromethane twice. The organic phase was dried over  $\text{Na}_2\text{SO}_4$ . After removing solvent under vacuum, the crude product was purified by silica column chromatography to give the title compound as a white solid in 75% yield.  $^1\text{H NMR}$  ( $\text{CDCl}_3$ , ppm): 3.61 (t,  $J = 7.2$  Hz, 2H), 1.65 (m, 2H), 1.31 (m, 10H), 0.89 (t,  $J_1 = 6.2$  Hz,  $J_2 = 6.9$  Hz, 3H). HRMS (ESI) ( $M^+$ ,  $\text{C}_{14}\text{H}_{17}\text{Br}_2\text{NO}_2\text{S}$ ): calcd, 420.9347; found, 420.9341.

**Synthesis of PDTC.** In a 25 mL round bottom flask, monomer 2 (254 mg, 0.35 mmol) and 7 (134 mg, 0.32 mmol) were charged with a condenser under  $\text{N}_2$  protection. Then, dry toluene (3 mL), DMF (0.5 mL) and  $\text{Pd}(\text{PPh}_3)_4$  (7 mg) were added into the flask consequently. The resulting mixture was degassed twice and heated in a microwave reactor with 100 °C for 10 min, 120 °C for 50 min. After cooling to room temperature, the mixture was poured into methanol. The precipitate was collected and washed with acetone for 24 h with a Soxhlet apparatus. Further purification was performed in a preparative GPC using THF as the mobile phase. The recovered black solid from THF solution was collected and dried overnight under vacuum (130 mg, 62%).  $^1\text{H NMR}$  (500 MHz,  $\text{CDCl}_3$ ,  $\delta$ ) 8.07–7.99 (m, 2H), 3.75 (br, 2H), 2.04 (br, 3H), 1.76 (br, 2H), 1.41–1.29 (m, 10H), 1.05–0.69 (m, 34H).  $M_n = 16.0$  kDa,  $M_w = 20.2$  kDa, PDI = 1.26.

**Synthesis of PDTSi.** PDTSi was synthesized with monomer 4 (280 mg, 0.37 mmol) and 7 (136 mg, 0.32 mmol) by following

a similar procedure to that of PDTC (120 mg, 55%).  $^1\text{H NMR}$  (500 MHz,  $\text{CDCl}_3$ ,  $\delta$ ) 8.12–7.98 (m, 2H), 3.73 (br, 2H), 2.05 (br, 2H), 1.74–0.80 (m, 47H).  $M_n = 13.6$  kDa,  $M_w = 19.4$  kDa, PDI = 1.43.

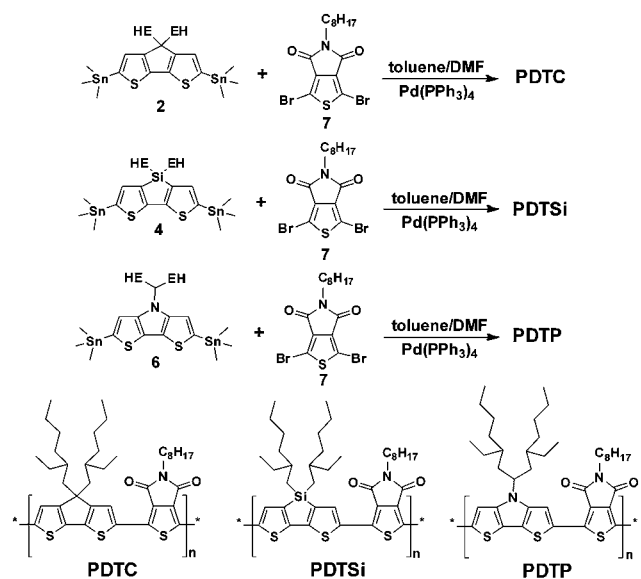
**Synthesis of PDTP.** PDTP was synthesized with monomer 6 (240 mg, 0.32 mmol) and 7 (127 mg, 0.30 mmol) by following a similar procedure to that of PDTC (110 mg, 54%).  $^1\text{H NMR}$  (500 MHz,  $\text{CDCl}_3$ ,  $\delta$ ) 8.39 (br, 2H), 4.64 (br, 1H), 3.74 (br, 2H), 2.24 (br, 2H), 1.74–0.76 (m, 47H).  $M_n = 10.6$  kDa,  $M_w = 13.7$  kDa, PDI = 1.29.

### 3. Results and discussion

#### Synthesis

Scheme 1 shows the synthesis of the dithiophene-based monomers. Compound 1 was prepared from the alkylation of 4*H*-cyclopenta[2,1-*b*:3,4-*b'*]dithiophene using 2-ethylhexylbromide in the presence of DMSO and aqueous KOH.<sup>31</sup> Direct lithiation of compound 1 to remove  $\alpha$ -H of the thiophene unit at –78 °C and subsequent quenching with trimethyltin chloride gave the corresponding di(trimethyl)stannyl compound 2 in 67% yield. The synthesis of compound 3 involves the double halogen–lithium exchange of bromine in 3,3'-dibromo-5,5'-bis-(trimethylsilyl)-2,2'-bithiophene using *n*-BuLi and subsequent ring closure by adding di(2-ethylhexyl)dichlorosilane.<sup>17</sup> Then, a similar procedure used to make compound 2 was employed to give compound 4 in 77% yield. Compound 5 was prepared from 4,4'-dibromo-2,2'-bithiophene by the ring cyclization using a mixture of  $\text{Pd}_2(\text{dba})_3$  and BINAP as catalyst.<sup>25</sup> After careful purification, the corresponding stannyl compound 6 was achieved by direct lithiation using *t*-BuLi and quenching with trimethyltin chloride in 75% yield. The further purification of compounds 2, 4 and 6 through silica (or alumina) column chromatography will lead to significant decomposition to the compounds 1, 3 and 5, respectively. Compound 7 was made from multiple steps starting from 3,4-dibromothiophene using the literature reported method.<sup>27,32</sup>

The polymers were synthesized by reacting the corresponding bis-stannyl compounds (2, 4 and 6) with 7 under the Stille polymerization conditions using toluene–DMF as mixed solvents and  $\text{Pd}(\text{PPh}_3)_4$  as catalyst under microwave heating (Scheme 2). The resulting crude polymers were purified by Soxhlet extraction with methanol and acetone, successively, to remove low molecular weight oligomers and residual catalyst. The collected polymers were further purified by preparative GPC using THF as the moving phase. The final polymers were collected by precipitating into methanol, filtered and dried under vacuum. The polymers show good solubility in common organic solvents such as chloroform, THF, chlorobenzene, and dichlorobenzene. The molecular weights of the polymers were determined by GPC against the polystyrene standard (Table 1). The number-average molecular weights ( $M_n$ ) of PDTC, PDTSi, and PDTP are 16.0 kDa, 13.6 kDa and 10.6 kDa, respectively, with polydispersity indexes (PDI) of 1.26, 1.43 and 1.29. Thermal properties of these polymers were evaluated with differential scanning calorimetry (DSC). The samples were heated at 10 °C  $\text{min}^{-1}$  under nitrogen. The DSC scan of PDTC showed a clear



Scheme 2 Synthesis of polymers PDTC, PDTSi and PDTP.

glass transition at  $\sim 180$  °C, however, PDTSi and PDTP did not show any transitions between 20 and 350 °C.

### Optical properties

Optical properties of these polymers were investigated in their chloroform solutions and in thin films. Fig. 1a shows the absorption spectra of all three polymers in chloroform. It can be seen from the spectra that the absorption maximum changes from 653 nm in PDTC with a high-energy shoulder at 604 nm, to 608 nm in PDTSi with a low-energy shoulder at 660 nm, and to 645 nm in PDTP with a high-energy shoulder at 598 nm. The absorption edge of PDTC and PDTSi are similar at  $\sim 723$  nm, while PDTP has a lower-energy absorption edge at 747 nm. In the thin film state (Fig. 1b), the predominant peaks move to 671, 665, and 686 nm in PDTC, PDTSi and PDTP, respectively. The red-shift of absorption in the thin film state implies a slightly increased  $\pi$ - $\pi$  stacking between polymer chains. On the other hand, the slight red-shift of the  $\lambda_{\text{max}}$  of PDTP is consistent with the stronger electron-donating properties of the N atom compared to either C or Si atoms.<sup>25</sup> The absorption edges of PDTC, PDTSi and PDTP in their film state are 741, 734 and 778 nm, respectively. The corresponding optical bandgaps of these polymers were estimated to be 1.67, 1.70 and 1.59 eV for PDTC,

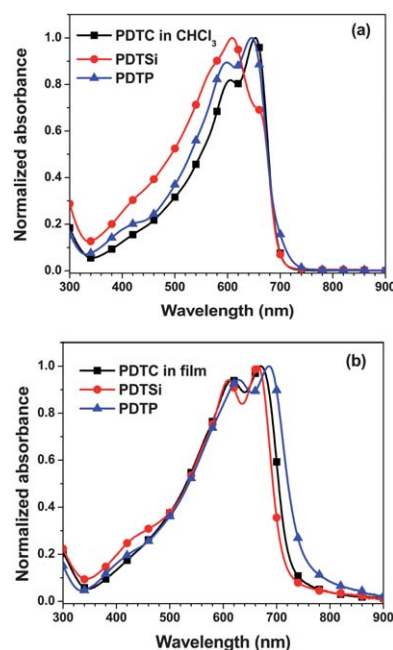


Fig. 1 UV-Vis spectra of polymers PDTC, PDTSi and PDTP in (a) chloroform solution and in (b) film states.

PDTSi and PDTP, respectively by calculating from the absorption edge of these films (Table 1).

### Electrochemical properties

To investigate the oxidative and reductive behaviors of these polymers, cyclic voltammograms (CVs) were performed for thin films prepared from these polymers on ITO with a Pt counter electrode and a Ag/Ag<sup>+</sup> reference electrode in 0.1 M tetrabutylammonium hexafluorophosphate in MeCN at a scan rate of 100 mV s<sup>-1</sup>. The HOMO and LUMO energy levels were calculated using the equations<sup>33</sup>

$$\text{HOMO} = -[E_{\text{ox}} - E_{\text{ferrocene}} + 4.80] \text{ eV}$$

$$\text{LUMO} = -[E_{\text{red}} - E_{\text{ferrocene}} + 4.80] \text{ eV}$$

where  $E_{\text{ox}}$  and  $E_{\text{red}}$  are the onset of the oxidation and reduction potential, respectively.  $E_{\text{ferrocene}}$  is the onset of the oxidation

Table 1 Molecular weight, PDI, thermal, optical and electrochemical data of polymers PDTC, PDTSi and PDTP

Polymer	$M_n/\text{kg mol}^{-1a}$	PDI	UV-Vis absorption				Cyclic voltammetry		
			solution		film		HOMO/eV	LUMO/eV	Band-gap
			$\lambda_{\text{max}}/\text{nm}$	$\lambda_{\text{onset}}/\text{nm}$	$\lambda_{\text{max}}/\text{nm}$	$\lambda_{\text{onset}}/\text{nm}$			
PDTC	16.0	1.26	653; 604	724	671; 616	741	-5.43	-3.76 <sup>b</sup> /-3.25 <sup>c</sup>	1.67 <sup>d</sup> /2.18 <sup>e</sup>
PDTSi	13.6	1.43	660; 608	723	665; 609	734	-5.44	-3.74 <sup>b</sup> /-3.17 <sup>c</sup>	1.70 <sup>d</sup> /2.27 <sup>e</sup>
PDTP	10.6	1.29	645; 598	747	686; 628	778	-5.16	-3.57 <sup>b</sup> /-3.08 <sup>c</sup>	1.59 <sup>d</sup> /2.08 <sup>e</sup>

<sup>a</sup> Determined by GPC against polystyrene standard. <sup>b</sup> Calculated from the optical band-gap. <sup>c</sup> Measured from cyclic voltammetry. <sup>d</sup> Optical band-gap. <sup>e</sup> Electrochemical band-gap.

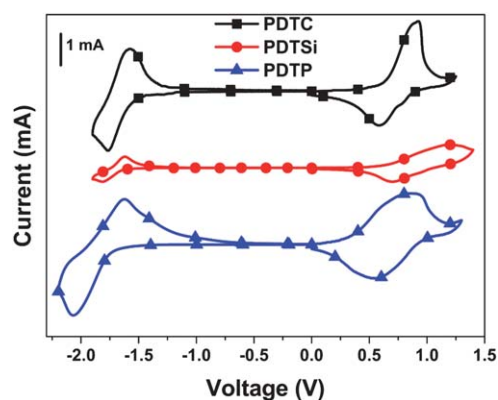


Fig. 2 CV curves of polymers.

potential of ferrocene. Fig. 2 shows the CV curves of the polymers and the detailed data are summarized in Table 1. As a comparison, the LUMO levels of these polymers were also calculated from the HOMO levels measured from CV and the optically measured bandgaps. The HOMO energy levels measured by CV for PDTC, PDTSi, and PDTP are  $-5.43$ ,  $-5.44$  and  $-5.16$  eV, respectively, which are  $0.20$ – $0.60$  eV lower than those reported for C- or Si-bridged bithiophene-based polymers.<sup>15,17</sup> The LUMO energy levels measured by CV are  $-3.25$ ,  $-3.17$  and  $-3.08$  eV, respectively. However, the calculated LUMO energy levels (the difference between HOMO and  $E_{\text{gopt}}$ ) are  $-3.76$ ,  $-3.74$  and  $-3.57$  eV, respectively, thus the electrochemical band-gap ( $E_{\text{gec}}$ ) is larger than the optical band-gap  $E_{\text{gopt}}$ . Similar phenomena have been reported in C- and Si-bridged bithiophene-based polymers.<sup>17,22–26</sup>

Usually, the bandgap and HOMO/LUMO energy levels originate from the molecular orbital hybridization of donor and acceptor energy levels in the donor–acceptor type polymers. Therefore, electron-donating groups will reduce  $E_{\text{g}}$  by raising the HOMO energy level in the polymer. In our case, the cyclopentadithiophene donor unit in PDTC and dithienosilole donor unit in PDTSi should have similar electron-donating abilities due to their similar experimental bandgaps and energy levels (Fig. 2, Table 1). However, in the PDTP polymer, the electron-donating ability of N atom is much stronger than both C and Si atoms, therefore, a lower bandgap and a higher HOMO energy level for this polymer were found.<sup>25</sup>

In BHJ photovoltaic cells, the proper energy offset between LUMO of donor and acceptor is required to provide energetically favorable condition for exciton dissociation.<sup>34</sup> As shown in Table 1, the difference between the LUMO levels of three polymers and PC<sub>71</sub>BM ( $-4.30$  eV) is between  $0.54$  and  $0.73$  eV, which is sufficient for achieving efficient exciton dissociation from the interface of the polymer donor and PC<sub>71</sub>BM acceptor. In addition,  $V_{\text{oc}}$  is proportional to the energy offset between the HOMO energy level of the polymer donor and the LUMO energy level of fullerene derivatives. Therefore, in the polymer/PCBM system, a deeper HOMO energy level will lead to higher  $V_{\text{oc}}$ . As discussed above, the deeper HOMO levels of these polymers compared to other bithiophene-based polymers ( $-5.4$  vs.  $-5.1$  eV) give higher  $V_{\text{oc}}$  in BHJ photovoltaic cells and ultimately lead to improved efficiency.

To better understand the oxidative and reductive properties of these polymers, the electronic properties of their trimer model

compounds were calculated by Density Functional Theory (DFT) at the B3LYP/6-31G(d) level. The HOMO and LUMO wave functions of the trimer model compounds are shown in Fig. 3. It is noted that all side-chain substituents were replaced with ethyl groups to save calculation time since this simplification only has a minimal effect on the electronic properties. The calculation for HOMO showed nice delocalization along the whole conjugated backbone affected by both donor and acceptor parts. Similarly, the calculated density of states for LUMO also showed a nice distribution across the whole conjugated backbone, but with more effect on the acceptor part. In addition, the effects of the bridging atom in the dithiophene unit are quite discrete for both the HOMO and LUMO electron density distributions. The densities of the respective HOMO wave functions are distributed across the fused hetero-aromatic backbones with less density on the electron-accepting substituents. For the LUMO, electron densities are localized to a greater degree on the respective electron acceptor units and at the center of the fused aromatic backbone. A final observation about the phases of the atomic contributions at the double bonds to both frontier MOs is warranted: in the HOMO wave function, the carbon–carbon double bond units are  $\pi$ -bonding with alternating phase with respect to adjacent double bonds. In the LUMO, however, the former carbon–carbon double bond units are  $\pi^*$  and have the same phase as their neighbors. These results show that both the donor and acceptor in these D–A polymers can significantly affect the energy levels.

### OFET properties

Carrier mobility also plays an important role in the performance of BHJ PSCs and a carrier mobility of larger than  $10^{-4}$  cm<sup>2</sup> V<sup>-1</sup> s<sup>-1</sup> is needed for the polymer donor. To measure hole mobility, top contact organic field-effect transistors (OFET) coated with these polymers were fabricated using gold as the source and drain electrodes. Interdigitated source (s) and drain (d) electrodes ( $W = 9000$   $\mu\text{m}$ ,  $L = 90$   $\mu\text{m}$ ,  $W/L = 100$ ) were defined on top of the polymer by evaporating a 50 nm thick gold film through a shadow mask. The saturation field-effect mobility ( $\mu$ ) was calculated from the following equation:

$$I_{\text{ds}} = (W/2L)\mu C_i (V_{\text{gs}} - V_{\text{th}})^2$$

where  $W$  and  $L$  are the channel width and length, respectively.  $C_i$  is the capacitance of the insulating SiO<sub>2</sub> layer per unit,  $V_{\text{gs}}$  and  $V_{\text{th}}$  are the gate voltage and the threshold voltage, respectively.<sup>34</sup>

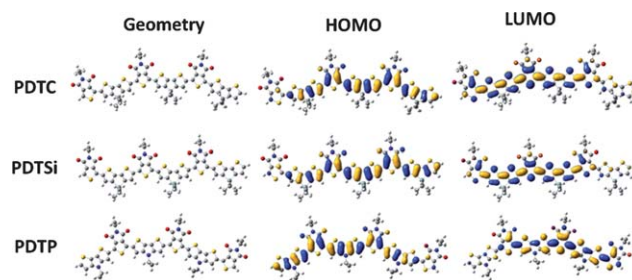


Fig. 3 The HOMO and LUMO wave functions of the trimer model of polymers PDTC, PDTSi and PDTP.

Fig. 4 shows the FET characteristics of the devices in p-channel mode with PDTC, PDTSi and PDTP as the channel materials. The hole-mobility of the polymer was calculated from the transport characteristics of the FETs by plotting  $I_{ds}$  with respect to  $V_{gs}$ . The calculated hole-mobilities of PDTC, PDTSi and PDTP are  $1.50 \times 10^{-3}$ ,  $6.0 \times 10^{-4}$  and  $3.9 \times 10^{-4} \text{ cm}^2 \text{ V}^{-1} \text{ s}^{-1}$ , respectively, with the on/off ratios of  $10^4$ – $10^5$ . These values are within the desirable range for OPV applications and also indicate that there exists significant intramolecular charge transfer or  $\pi$ - $\pi$  packing in these polymer films.

### Photovoltaic properties

The photovoltaic properties of these polymers were investigated using a standard device configuration of ITO/PEDOT:PSS/polymer:PC<sub>71</sub>BM (1 : 2)/Ca/Al and their performance were measured under 100 mW cm<sup>-2</sup> AM 1.5 illumination. The active layers of

these polymers were first prepared from spin-coating their *o*-dichlorobenzene (*o*-DCB) solutions and the corresponding devices were fabricated and measured. The photovoltaic performance including  $V_{oc}$ ,  $J_{sc}$ , FF, and PCE are summarized in Table 2. The  $J$ - $V$  curves are shown in Fig. 6a. For the PDTC device, the result showed a PCE of 3.74%. Under the same conditions, PCE of 1.18% and 0.91% were obtained for PDTSi and PDTP, respectively. It is worth noting that these devices show quite high  $V_{oc}$  (up to 0.91 V in the PDTSi device), which is  $\sim 0.2$ – $0.4$  V higher than other devices made from C, Si and N-bridged dithiophene polymers.<sup>10,17,22–26</sup> The high  $V_{oc}$  obtained in these devices are the result from the low HOMO energy level of these polymers ( $-5.43$  eV for PDTC,  $-5.44$  eV for PDTSi, and  $-5.16$  eV for PDTP).<sup>35</sup>

In general, the formation of a bicontinuous interpenetrating network between polymer donor and PCBM acceptor is the most promising architecture in BHJ cells. The morphology of the active layer (polymer:PCBM blend film) is very critical for the performance of BHJ cells. If there are large size domains and significant phase separation in the active layer, it will reduce the interfaces for efficient charge separation and a smooth film with few domains will also increase the possibility for charge recombination. As can be seen from Table 2, PDTSi and PDTP devices fabricated from *o*-DCB solution show much poorer performance compared to the PDTC device. The inferior device performance may be due to the non-optimal morphology in these polymer/PC<sub>71</sub>BM blend films.

To understand the morphological effect on the device performance, the films of polymer blends were investigated by tapping-mode atomic force microscopy (AFM) and these AFM topography images are shown in Fig. 5. As shown in Fig. 5a, the PDTC/PC<sub>71</sub>BM film shows a smoother surface and smaller phase separation, which facilitates charge separation and results in higher device performance. However, in the PDTSi/PC<sub>71</sub>BM and PDTP/PC<sub>71</sub>BM blend films (Fig. 5b, c), significant phase separation and large domains were observed. This leads to poorer charge separation and increased charge carrier recombination. The strong phase separation may be due to polymer self-aggregation and/or incompatibility between the polymer and PC<sub>71</sub>BM. Therefore, this results in poorer performance in PDTSi and PDTP devices.

There are several ways to alter the interpenetrating nanoscale morphology of a BHJ cell. Bazan *et al.* have demonstrated that the addition of a small amount of solvent additives with high boiling point into the conjugated polymer/PCBM solution during processing can give a substantial increase of device

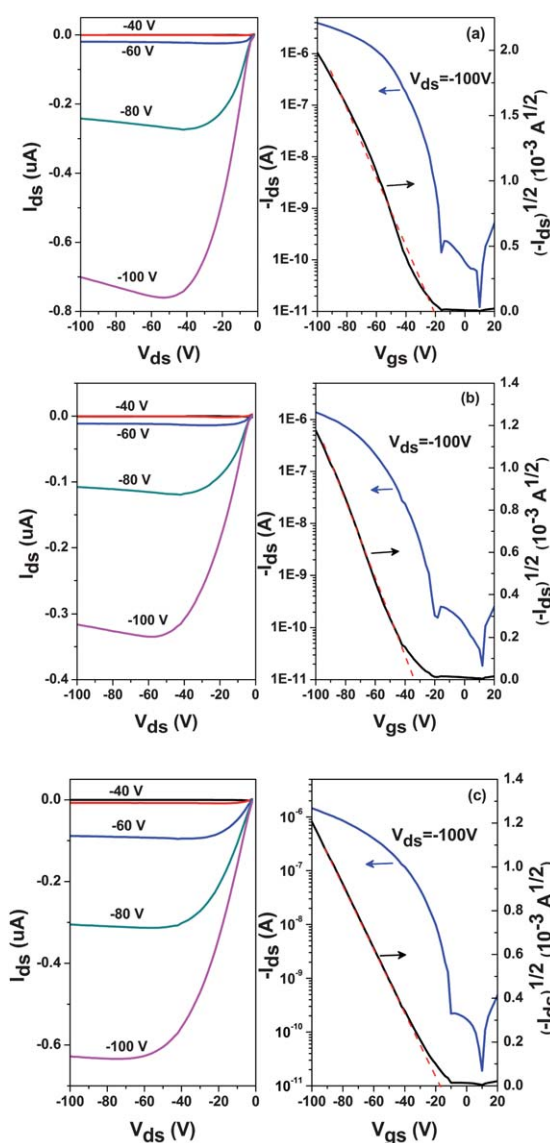
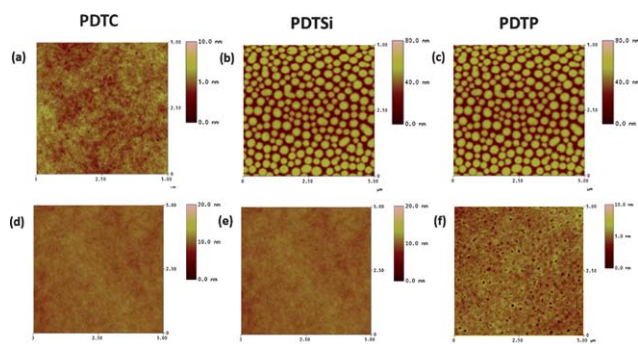


Fig. 4 The output at different gate voltage ( $V_{gs}$ ) and transfer characteristics in the saturation regime under constant source-drain voltage ( $V_{ds} = -100$  V) for PDTC (a), PDTSi (b) and PDTP (c).

Table 2 Performance of photovoltaic devices under AM 1.5 simulated illumination (100 mW cm<sup>-2</sup>)

Polymer:PC <sub>71</sub> BM (1 : 2)	$V_{oc}/V$	$J_{sc}/\text{mA cm}^{-2}$	FF	PCE (%)
PDTC <sup>a</sup>	0.80	10.04	0.47	3.74
PDTC <sup>b</sup>	0.80	9.40	0.45	3.45
PDTSi <sup>a</sup>	0.91	2.32	0.56	1.18
PDTSi <sup>b</sup>	0.85	6.58	0.37	2.13
PDTP <sup>a</sup>	0.71	2.53	0.50	0.91
PDTP <sup>b</sup>	0.76	4.69	0.53	1.69

<sup>a</sup> Film from pristine DCB. <sup>b</sup> Film from *o*-DCB : 2 vol% CN.



**Fig. 5** AFM topography images of polymer:PC<sub>71</sub>BM (1 : 2 wt) blend films from *o*-DCB (a, b, c) and *o*-DCB : 2 vol% 1-chloronaphthalene (d, e, f).

performance due to significantly improved morphology. The solvent additives play the role of slowing the aggregation of conjugated polymer and PCBM so as to be able to avoid forming the oversize polymer or PCBM aggregates, which inhibit charge carrier transport in the BHJ film.<sup>36,37</sup> Recently, 1-chloronaphthalene (CN) has been proved to be an alternative solvent additive in improving the performance of bridged dithiophene-based polymers.<sup>38,39</sup> To take advantage of this effect, CN was also used as the solvent additive to improve the morphology of the polymer blends, especially for the PDTSi/PC<sub>71</sub>BM and PDTC/PC<sub>71</sub>BM systems. The morphology of the polymer/PC<sub>71</sub>BM films cast from their *o*-DCB solution with 2 vol% of CN was studied by AFM. Fig. 5 shows the AFM topographical

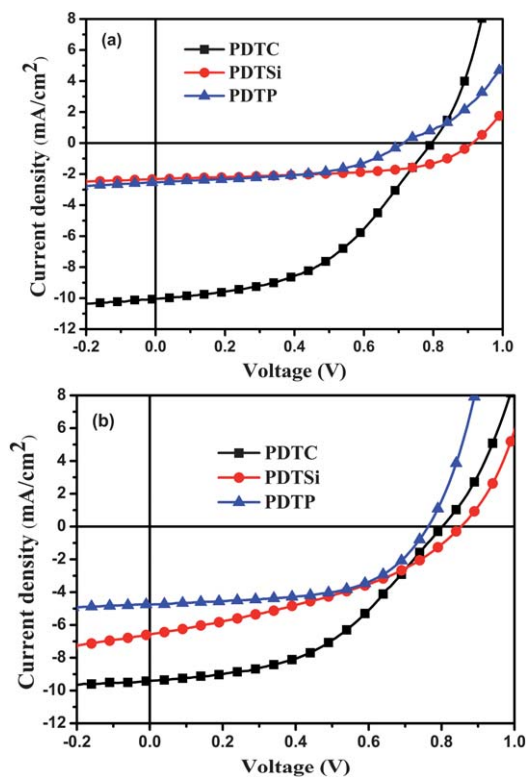


**Fig. 6**  $J$ - $V$  curves of PDTC, PDTSi and PDTP devices: (a) film prepared from pristine *o*-DCB solution and (b) film prepared from *o*-DCB:2 vol% 1-chloronaphthalene under illumination of AM 1.5, 100 mW cm<sup>-2</sup>.

images. As shown from Fig. 5d, the addition of 2 vol% CN had a minor effect on the morphology of the PDTC/PC<sub>71</sub>BM thin film. However, the previously observed large size domains from the PDTSi/PC<sub>71</sub>BM and PDTP/PC<sub>71</sub>BM thin films cast from their *o*-DCB solutions (Fig. 5b, c) can no longer be detected. The nanoscale morphologies of PDTSi/PC<sub>71</sub>BM and PDTP/PC<sub>71</sub>BM films were substantially improved. This indicates that CN solvent additive can promote the self-aggregation of PDTSi and PDTP in a relatively fluid medium and also improves the compatibility between polymer and PC<sub>71</sub>BM.<sup>37,38</sup> As a result, relatively smooth BHJ films of polymer/PC<sub>71</sub>BM were formed. To verify this point, BHJ cells with the same device configuration as described above were fabricated by spin-coating films from their *o*-DCB:2 vol% CN solutions. The optimized volume of CN is 2 vol%. The  $J$ - $V$  curves of these devices are shown in Fig. 6b and summarized in Table 2. As shown in Fig. 6b, there are significant improvements in the device performance, especially for the PDTSi and PDTP devices. The PCE of the PDTC device remained at 3.45% while the PCE of the PDTSi device increased from 1.18% to 2.13% with almost 3 times increase of its  $J_{sc}$ . However,  $V_{oc}$  of the device showed a slight decrease to 0.85 V. A similar decrease has also been observed earlier<sup>10</sup> which may be due to morphological changes and interfacial interactions between the active layer and the cathode. For the PDTP device, the PCE improved from 0.91% to 1.69% after the addition of CN.

The external quantum efficiency (EQE) of these devices was measured to evaluate the photoresponse of the BHJ cells. Fig. 7 shows the EQE curves of the PDTC device fabricated from *o*-DCB and the PDTSi and PDTP devices fabricated from *o*-DCB:2 vol% CN solution. All devices exhibited efficient photoresponse between 350 and 750 nm. The EQE of the PDTC device is more than 45% with the highest value of 53.5% at 570 nm. However, the PDTSi and PDTP devices showed much lower EQE values compared to the PDTC device with their maxima at 38.3% and 25.2% at 560 nm, respectively. The low EQE values affect the low  $J_{sc}$  observed for PDTSi and PDTP devices (Table 2). In addition, the low EQE in PDTSi and PDTP devices was mainly ascribed to the lower hole mobility observed in these two polymers because of non-ideal interpenetrating nanoscale phase separation between the polymers and PC<sub>71</sub>BM. Since there are many factors affecting the phase separation, such as the

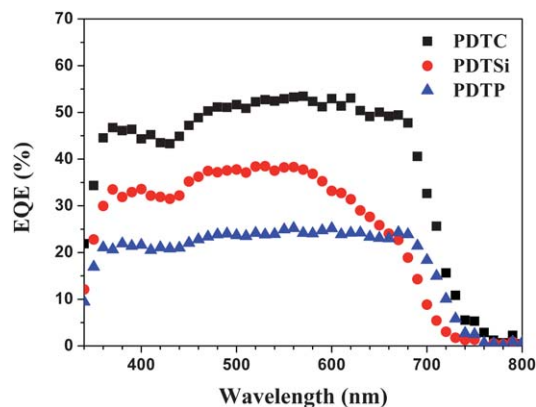


**Fig. 7** External quantum efficiency curves of optimized PDTC, PDTSi and PDTP devices.

Flory–Huggins interaction, the tendency of the components to aggregate, and kinetic constraints,<sup>10,40,41</sup> further work will focus on understanding the relationship between morphology and performance and will be reported elsewhere.

#### 4. Conclusion

Three new polymers, PDTC, PDTSi and PDTP, have been designed and synthesized through the Stille coupling polymerization between C-, Si-, N-bridged dithiophene stannyl compound and 1,3-dibromo-5-octylthieno[3,4-c]pyrrole-4,6-dione. The change from C, Si to N atom in the bridged dithiophene induces a red-shift in their thin film absorption spectra. The results from electrochemical measurements showed that these polymers possess lower HOMO levels (−5.44 eV for PDTSi, −5.43 eV for PDTC and −5.16 eV for PDTP) compared to previously reported analogs. These polymers also have good hole mobility (as high as  $1.50 \times 10^{-3}$ ) as measured by the FET technique. The photovoltaic properties of these polymers were investigated using the device configuration of ITO/PEDOT:PSS/polymer:PC<sub>71</sub>BM (1 : 2)/Ca/Al. The highest achievable PCE for PDTC, PDTSi, and PDTP is 3.74%, 2.13%, and 1.69%, respectively. It is worth noting that the  $V_{oc}$  of these devices increased significantly (~0.2–0.4 V) due to the lower HOMO energy level of these polymers compared to other C-, Si-, N-bridged dithiophene-based polymers.

#### Acknowledgements

The authors are grateful for the support of the National Science Foundation's STC program under DMR-0120967, the AFOSR's "Interface Engineering" Program (FA9550-09-1-0426), the DOE "Future Generation Photovoltaic Devices and Process" program (DE-FC3608GO18024/A000), the Office of Naval Research (N00014-08-1-1129) and the World Class University (WCU) program through the National Research Foundation of Korea under the Ministry of Education, Science and Technology (R31-10035). A. K.-Y. Jen thanks the Boeing-Johnson Foundation for financial support.

#### Notes and references

- C. J. Brabec, N. S. Sariciftci and C. J. Hummelen, *Adv. Funct. Mater.*, 2001, **11**, 15.
- F. C. Krebs, *Sol. Energy Mater. Sol. Cells*, 2009, **93**, 394.
- G. Dennler, M. C. Scharber and C. J. Brabec, *Adv. Mater.*, 2009, **21**, 1323.
- S. Gunes, H. S. Neugebauer and N. S. Sariciftci, *Chem. Rev.*, 2007, **107**, 1324.
- N. S. Sariciftci, L. Smilowitz, A. J. Heeger and F. Wudl, *Science*, 1992, **258**, 1474.
- G. Yu, J. Gao, J. C. Hummelen, F. Wudl and A. J. Heeger, *Science*, 1995, **270**, 1789.
- J. W. Chen and Y. Cao, *Acc. Chem. Res.*, 2009, **42**, 1709.
- Y. J. Cheng, S. H. Yang and C. S. Hsu, *Chem. Rev.*, 2009, **109**, 5868.
- G. Li, V. Shrotriya, J. Huang, Y. Yao, T. Moriarty, K. Emery and Y. Yang, *Nat. Mater.*, 2005, **4**, 864.
- J. Peet, J. Y. Kim, N. E. Coates, W. L. Ma, D. Moses, A. J. Heeger and G. C. Bazan, *Nat. Mater.*, 2007, **6**, 497.
- L. J. A. Koster, V. D. Mihailetschi and P. W. M. Blom, *Appl. Phys. Lett.*, 2006, **88**, 093511.
- E. G. Wang, L. Wang, L. F. Lan, C. Luo, W. L. Zhuang, J. B. Peng and Y. Cao, *Appl. Phys. Lett.*, 2008, **92**, 033307.
- Y. Y. Liang, Y. Wu, D. Q. Feng, S. T. Tsai, H. J. Son, G. Li and L. P. Yu, *J. Am. Chem. Soc.*, 2009, **131**, 56.
- Y. Y. Liang, D. Q. Feng, Y. Wu, S. T. Tsai, G. Li, C. Ray and L. P. Yu, *J. Am. Chem. Soc.*, 2009, **131**, 7792.
- R. C. Coffin, J. Peet, J. Rogers and G. C. Bazan, *Nat. Chem.*, 2009, **1**, 657.
- J. H. Hou, H. Y. Chen, S. Q. Zhang, R. I. Chen, Y. Yang, Y. Wu and G. Li, *J. Am. Chem. Soc.*, 2009, **131**, 15586.
- J. H. Hou, H. Y. Chen, S. Q. Zhang, G. Li and Y. Yang, *J. Am. Chem. Soc.*, 2008, **130**, 16144.
- J. Luo, H. B. Wu, C. He, A. Y. Li, W. Yang and Y. Cao, *Appl. Phys. Lett.*, 2009, **95**, 043301.
- C. He, C. M. Zhong, H. B. Wu, R. Q. Yang, W. Yang, F. Huang, G. C. Bazan and Y. Cao, *J. Mater. Chem.*, 2010, **20**, 2617.
- V. D. Mihailetschi, P. W. M. Blom, J. C. Hummelen and M. T. Rispen, *J. Appl. Phys.*, 2003, **94**, 6849.
- D. Mühlbacher, M. Scharber, M. Morana, Z. G. Zhu, D. Waller, R. Gaudiana and C. J. Brabec, *Adv. Mater.*, 2006, **18**, 2931.
- A. J. Moule, A. Tsami, T. W. Bünnagel, M. Forster, N. M. Kronenberg, M. Scharber, M. Koppe, M. Morana, C. J. Brabec, K. Meerholz and U. Scherf, *Chem. Mater.*, 2008, **20**, 4045.
- I. H. Jung, H. Kim, M. J. Park, B. Kim, J. H. Park, E. Jeong, H. J. Woo, S. Yoo and H. K. Shim, *J. Polym. Sci., Part A: Polym. Chem.*, 2010, **48**, 1423.
- M. C. Scharber, M. Koppe, J. Gao, F. Cordella, M. A. Loi, P. Denk, M. Morana, H. J. Egelhaaf, K. Forberich, G. Dennler, R. Gaudiana, D. Waller, Z. G. Zhu, X. B. Shi and C. J. Brabec, *Adv. Mater.*, 2010, **22**, 367.
- E. J. Zhou, M. Nakamura, T. Nishizawa, Y. Zhang, Q. S. Wei, K. Tajima, C. H. Yang and K. Hashimoto, *Macromolecules*, 2008, **41**, 8302.
- E. J. Zhou, Q. S. Wei, S. Yamakawa, Y. Zhang, K. Tajima, C. H. Yang and K. Hashimoto, *Macromolecules*, 2010, **43**, 821.
- Y. Zhang, H. K. Steven, H. L. Yip, Y. Sun, O. Acton and A. K. Y. Jen, *Chem. Mater.*, 2010, **22**, 2696.
- Y. P. Zou, A. Najari, P. Berrouard, S. Beaupre, B. R. Aich, Y. Tao and M. Leclerc, *J. Am. Chem. Soc.*, 2010, **132**, 5330.
- C. Piliego, T. W. Holcombe, J. D. Douglas, C. H. Woo, P. Beaujuge and J. M. J. Frechet, *J. Am. Chem. Soc.*, 2010, **132**, 7595.
- G. B. Zhang, Y. Y. Fu, Q. Zhang and Z. Y. Xie, *Chem. Commun.*, 2010, **46**, 4997.
- Z. G. Zhu, D. Waller, R. Gaudiana, M. Morana, D. Mühlbacher, M. Scharber and C. J. Brabec, *Macromolecules*, 2007, **40**, 1981.
- C. B. Nielsen and T. Bjornholm, *Org. Lett.*, 2004, **6**, 3381.
- J. Pommerehne, H. Vestweber, W. Guss, R. F. Mahrt, H. Bassler, M. Porsch and J. Daub, *Adv. Mater.*, 1995, **7**, 551.
- A. Zen, J. Pflaum, S. Hirschmann, W. Zhuang, F. Jaiser, U. Asawapirom, J. P. Rabe, U. Scherf and D. Neher, *Adv. Funct. Mater.*, 2004, **14**, 757.
- M. C. Scharber, D. Mühlbacher, M. Koppe, P. Denk, C. Waldauf, A. J. Heeger and C. J. Brabec, *Adv. Mater.*, 2006, **18**, 789.
- J. K. Lee, W. L. Ma, C. J. Brabec, J. Yuen, J. S. Moon, J. Y. Kim, K. Lee, G. C. Bazan and A. J. Heeger, *J. Am. Chem. Soc.*, 2008, **130**, 3619.
- J. S. Moon, C. J. Takacs, S. Cho, R. C. Coffin, H. Kim, G. C. Bazan and A. J. Heeger, *Nano Lett.*, 2010, **10**, 4005.
- C. V. Hoven, X. D. Dang, R. C. Coffin, J. Peet, T.-Q. Nguyen and G. C. Bazan, *Adv. Mater.*, 2010, **22**, E63.
- R. C. Coffin, J. Peet, J. Rogers and G. C. Bazan, *Nat. Chem.*, 2009, **1**, 657.
- H. Hoppe and N. S. Sariciftci, *J. Mater. Chem.*, 2006, **16**, 45.
- X. N. Yang and J. Loos, *Macromolecules*, 2007, **40**, 1353.